



Published in final edited form as:

Circulation. 2013 October 8; 128(15): . doi:10.1161/CIRCULATIONAHA.113.002624.

The Function and Distribution of Apolipoprotein A1 in the Artery Wall are Markedly Distinct from those in Plasma

Joseph A. DiDonato, PhD^{1,*}, Ying Huang, PhD^{1,*}, Kulwant Aulak, PhD¹, Orli Even-Or, PhD², Gary Gerstenecker, PhD^{1,3}, Valentin Gogonea, PhD^{1,3}, Yuping Wu, PhD⁴, Paul L. Fox, PhD¹, W.H. Wilson Tang, MD^{1,5}, Edward F. Plow, PhD⁶, Jonathan D. Smith, PhD^{1,5}, Edward A. Fisher, MD², and Stanley L. Hazen, MD PhD^{1,3,5}

¹Department of Cellular & Molecular Medicine, Lerner Research Institute, Cleveland Clinic, Cleveland, OH

²Department of Medicine, New York University, New York, NY

³Department of Chemistry, Cleveland State University, Cleveland, OH

⁴Department of Mathematics, Cleveland State University, Cleveland, OH

⁵Department of Cardiovascular Medicine, Heart and Vascular Institute, Cleveland Clinic, Cleveland, OH

⁶Department of Molecular Cardiology, Lerner Research Institute, Cleveland Clinic, Cleveland, OH

Abstract

Background—Prior studies show apolipoprotein A1 (apoA1) recovered from human atherosclerotic lesions is highly oxidized. *Ex vivo* oxidation of apoA1 or high density lipoprotein (HDL) cross-links apoA1 and impairs lipid binding, cholesterol efflux and lecithin cholesterol acyltransferase (LCAT) activities of the lipoprotein. Remarkably, no studies to date directly quantify either the function or HDL particle distribution of apoA1 recovered from the human artery wall.

Methods and Results—A monoclonal antibody (mAb 10G1.5) was developed that equally recognizes lipid-free and HDL-associated apoA1 in both native and oxidized forms. Examination of homogenates of atherosclerotic plaque-laden aorta showed >100-fold enrichment of apoA1 compared to normal aorta ($P < 0.001$). Surprisingly, buoyant density fractionation revealed only a minority (<3% of total) of apoA1 recovered from either lesions or normal aorta resides within an HDL-like particle ($d = 1.063 - 1.21$). In contrast, the majority (>90%) of apoA1 within aortic tissue (normal and lesions) was recovered within the lipoprotein-depleted fraction ($d > 1.21$). Moreover, both lesion and normal artery wall apoA1 is highly cross-linked (50–70% of total), and functional characterization of apoA1 quantitatively recovered from aorta using mAb 10G1.5 showed ~80% lower cholesterol efflux activity and ~90% lower LCAT activity relative to circulating apoA1.

Correspondence: Joseph DiDonato, PhD, 9500 Euclid Avenue, NE-10, Cleveland, OH 44195, Phone: 216-445-2174, Fax: 216-636-0392, didonaj@ccf.org, or, Stanley L Hazen, MD, PhD, 9500 Euclid Avenue, NE-10, Cleveland, OH 44195, Phone: 216-445-9763, Fax: 216-444-9404, hazens@ccf.org.

*Co-first authors

Publisher's Disclaimer: This is a PDF file of an unedited manuscript that has been accepted for publication. As a service to our customers we are providing this early version of the manuscript. The manuscript will undergo copyediting, typesetting, and review of the resulting proof before it is published in its final citable form. Please note that during the production process errors may be discovered which could affect the content, and all legal disclaimers that apply to the journal pertain.

Conflict of Interest Disclosures: The remaining authors have no disclosures to report.

Conclusions—The function and distribution of apoA1 in human aorta are quite distinct from those found in plasma. The lipoprotein is markedly enriched within atherosclerotic-plaque, predominantly lipid-poor, not associated with HDL, extensively oxidatively cross-linked, and functionally impaired.

Keywords

plaque; apolipoproteins; arteriosclerosis; cardiovascular diseases

INTRODUCTION

The poor performance of several recent clinical trials targeting elevation of high density lipoprotein (HDL) cholesterol^{1–3}, and the recent Mendelian genetic studies questioning a causal link between genetic variants controlling HDL cholesterol levels and cardiovascular disease risk⁴, argue for a reappraisal of our understanding of HDL. Such a reappraisal demands that we question assumptions about the pathobiology of the lipoprotein, particularly where direct investigation is lacking. Much of what is known biologically about apoA1 in human studies comes from investigations employing isolated lipoprotein particles from the circulation (plasma or serum) using buoyant density ultracentrifugation. A known exchangeable lipoprotein, it is widely recognized that the vast majority of apoA1 within the circulation resides on spherical HDL particles where it serves as the major structural protein of a complex macromolecular assembly of lipoprotein particles with defined buoyant density (1.063 d 1.21)⁵. An unproven assumption is that the numerous biological functions observed with HDL or apoA1 recovered from the circulation will mirror what occurs elsewhere in vivo.

The functional properties of apoA1 and HDL within the circulation, however, may not faithfully reflect what occurs within the artery wall. Early studies identified that lipoproteins isolated from the artery wall, particularly LDL, undergo assorted alterations including proteolysis, various oxidative modifications and lipolysis to varying extents^{6, 7}. Several years ago we reported that apoA1 recovered from human atherosclerotic arterial lesions was selectively targeted for oxidative modification by myeloperoxidase (MPO)-generated and nitric oxide (NO)-derived oxidants, and that oxidative modification of apoA1 and HDL *ex vivo* to a comparable extent resulted in loss of cholesterol efflux activity of the lipoprotein⁸. Parallel functional characterization and mass spectrometry studies of circulating HDL isolated by buoyant density ultracentrifugation revealed that higher apoA1 content of oxidative modifications specifically formed by MPO- and NO-derived oxidants was associated with impairment in plasma membrane transporter ATP-binding cassette A1 (ABCA1)-dependent cholesterol efflux function of the lipoprotein⁸, lecithin cholesteryl acyl transferase (LCAT) activity and acquisition of pro-inflammatory activity^{9, 10}. Similar findings have been replicated by other groups^{11, 12}, and numerous additional proteomics studies have since mapped site-specific oxidative modifications to apoA1 recovered from the human artery wall^{13–16}. These studies collectively reveal that apoA1 is extensively oxidatively modified within an atherosclerotic-laden artery wall, and similar oxidative modifications to the lipoprotein *ex vivo* are associated with pro-atherogenic changes in apoA1 function. Of note, however, no studies to date have directly examined the functional properties or the particle distribution of apoA1 recovered from human artery wall. The paucity in direct functional characterization studies is likely a result of the significant challenges that exist in obtaining sufficient quantities of fresh human arterial tissue for such biochemical and biological studies.

Herein we sought to examine both the distribution and the functional properties of apoA1 recovered from the human artery wall. The present studies demonstrate multiple remarkable

findings, including direct evidence that the biological function and HDL particle distribution of apoA1 within both normal and atherosclerosis-laden human aortic tissues is markedly distinct from that of circulating apoA1 and HDL. These studies suggest that the historical focus thus far on circulating HDL cholesterol levels may not adequately reflect what is going on with regard to apoA1 function and HDL particle distribution within the artery wall.

MATERIALS AND METHODS

Materials

D₂O was purchased from Cambridge Isotopes, Inc (Andover, MA). Chelex-100 resin, fatty acid-free bovine serum albumin (BSA) and crystalline catalase (from bovine liver; thymol-free) were purchased from Boehringer-Mannheim (Ridgefield, CT). Sodium phosphate, H₂O₂ and NaOCl were purchased from Fisher Chemical Company (Pittsburgh, PA). Commercial apoA1 antibodies were from Abcam (Cambridge, MA), Santa Cruz Biotechnologies (South San Francisco, CA), and Genway/Sigma (St. Louis, MO). 1,2-dimyristoyl-*sn*-glycero-3-phosphoethanolamine-N-(7-nitro-2-1,3-benzoxadiazol-4-yl) (NBD-PE), was purchased from Avanti Polar Lipids. All other materials were purchased from Sigma Chemical Company (St. Louis, MO) except where indicated.

Methods

General Procedures—Circulating HDL and plasma-derived apoA1 purified were obtained from healthy volunteer donors who gave written informed consent and the Institutional Review Board of the Cleveland Clinic approved the study protocol. Mouse studies involving monoclonal antibody generation were performed under protocols approved by the Institutional Animal Care and Use Committee at the Cleveland Clinic. Lipoproteins, including HDL and HDL-like particles (1.063 d 1.21) from plasma and tissue homogenates, respectively, were isolated by sequential buoyant density ultracentrifugation at low salt concentrations using D₂O/sucrose¹⁷. Protein concentrations were determined by Markwell modified protein assay with bovine serum albumin as standard. Human apoA1 used as control for cholesterol efflux and LCAT activity assays was purified as described¹⁸. Reconstituted HDL (rHDL) from isolated apoA1 was prepared by cholate dialysis method¹⁹ employing a molar ratio of apoA1:POPC:cholesterol of 1:100:10. HDL particles were further purified by gel filtration chromatography using a Sephacryl S300 column (GE Healthcare, Waukesha, WI) on a Bio-Rad Biologics DuoFlo FPLC (Bio-Rad, Hercules, CA). Myeloperoxidase (MPO) (donor: hydrogen peroxide, oxidoreductase, EC 1.11.1.7) was isolated (final A430/A280 ratio of 0.6) as described^{8, 13, 14} and its concentration was determined spectrophotometrically ($\epsilon_{430} = 170 \text{ mM}^{-1} \text{ cm}^{-1}$)^{8, 13, 14}. H₂O₂ and ⁻OCl concentrations were each determined spectrophotometrically ($\epsilon_{240} = 39.4 \text{ M}^{-1} \text{ cm}^{-1}$;²⁰ and $\epsilon_{292} = 350 \text{ M}^{-1} \text{ cm}^{-1}$;^{8, 13, 14}, respectively) prior to use. Peroxynitrite (ONOO⁻) was purchased from Cayman Chemicals (Ann Arbor, MI), and quantified spectrophotometrically prior to use ($\epsilon_{302} = 1.36 \text{ mM}^{-1} \text{ cm}^{-1}$)^{13, 14}. All buffers used were passed through a Chelex-100 column and supplemented with 100 μM diethylenetriaminepentaacetic acid (DTPA) to remove any trace levels of redox-active metals. All glassware used was rinsed with 100 μM DTPA, pH 7.4, then Chelex-100 treated distilled deionized H₂O, and baked at 500°C prior to use. Sodium dodecyl sulfate-polyacrylamide gel electrophoresis (SDS-PAGE) was performed as described¹³.

Tissue Collection—Fresh surgical specimens of human aortic tissue were obtained as discarded material, both at time of organ harvest from transplant donors and during valve/aortic arch ("elephant trunk") replacement surgery. Tissue was immediately rinsed in ice-cold normal saline until free of visible blood, submerged in argon-sparged 65 mM sodium phosphate buffer (pH 7.4) supplemented with 100 μM DTPA and 100 μM butylated

hydroxytoluene (BHT), and stored at -80°C in screw cap specimen containers in which headspace was purged with argon. BHT was omitted from buffer in specimens where apoA1 was isolated for functional activity assays.

Monoclonal antibody (mAb) 10G1.5 generation, specificity and labeling—

Hybridoma cell lines were generated by immunizing apoA1 $^{-/-}$ mice with purified delipidated human apoA1 isolated from HDL recovered from healthy donors. Amongst the positive clones, subclones were screened until a monoclonal antibody (mAb) with desired binding specificity for equal recognition of all forms of apoA1 (see below) was identified. The subclone, mAb 10G1.5, was selected by screening for equal recognition of lipid-free and lipidated (in rHDL) apoA1 under native conditions, as well as following oxidation by exposure to multiple different systems including MPO/H₂O₂/Cl⁻, MPO/H₂O₂/NO₂⁻, and CuSO₄ (oxidized as outlined below). To produce sufficient levels of 10G1.5 for immune-affinity purification of apoA1 from arterial tissues, hybridoma clones were injected into pristane-treated male BALB/c mice (8 weeks of age). Ascites fluid was collected, precipitated with ammonium sulfate, then bound and eluted from a protein A/G column (Thermo Scientific Pierce, Rockford, IL) to purify mouse monoclonal antibodies. Isotypes of the mAbs were determined with the mouse mAb isotyping kit (Catalog# 26179, Pierce Rapid Antibody Isotyping Strips plus Kappa and Lambda – Mouse, Thermo Scientific Pierce, Rockford, IL).

Specificity of mAb 10G1.5 was tested using apoA1 or rHDL either in native form, or following incubation at 37°C in 60 mM Na[PO₄] buffer (pH 7.4) with multiple different oxidation systems. The different MPO systems consisted of 19 nM MPO, 100 μM DTPA, 40 μM H₂O₂ and either 100 mM NaCl or 1 mM KBr or 1mM NaNO₂ as indicated. Horseradish peroxidase (HRP 19 nM) was used with 40 μM H₂O₂. ApoA1 and rHDL were exposed to MPO and HRP for 90 min at 37°C and the reactions were stopped by addition of 2mM methionine and 300 nM catalase. All other oxidation reactions were carried out for 24 hrs at 37°C . Final concentrations of oxidants used were: H₂O₂, 40 μM ; ONOO⁻, 40 μM ; ONOO⁻/HCO₃⁻ (40 μM each); CuSO₄, 10 μM ; CuSO₄/H₂O₂ (10 μM and 40 μM , respectively); FeCl₃, 10 μM ; FeCl₃/H₂O₂ (10 μM and 40 μM , respectively). ApoA1 or rHDL (prepared from apoA1 or their various oxidized versions) were coated at 0.5 $\mu\text{g}/\text{ml}$ into EIA plates and probed with 10 ng/mL anti-totalapoA1 monoclonal antibody 10G1.5 at room temperature for 1 h. For Western blot analyses, mAb 10G1.5 was IRDye labeled (LI-COR Biosciences, Lincoln NE) by using LI-COR IRDye 800CW high molecular kit at a dye/protein ratio at 4:1, and visualized by infrared imaging. The IRDye 800CW dye bears an N-hydroxysuccinimide ester reactive group that couples to free amino groups on the antibody, forming a stable conjugate with antibody. Coupling was performed as per the manufacturer's instructions.

Human apoA1 quantification—Human apoA1 was quantified by an FDA approved apoA1 immunoassay on the Abbott ARCHITECT ci8200 Integrated Analyzer System (Abbott Labs, Abbott Park, IL). All other apoA1 was quantified by quantitative immunoblot analysis using mAb 10G1.5 as the detecting antibody, as determined against a standard curve of known purified apoA1 standard. Immuno-reactive bands were quantified using Image Studio software (version 2, LI-COR) or Image J (version 1.46, <http://rsbweb.nih.gov/>). All nascent HDL particles, and isolated human HDL2 and HDL3, were further purified by gel filtration chromatography using a Sephacryl S300 column (GE Healthcare, Waukesha, WI) on a Bio-Rad Biologics DuoFlo FPLC.

Aortic tissue homogenization—Atherosclerotic lesions from aortic tissues were from subjects (n>20) of an average age of 83yr \pm 3yr. Normal human aortic tissues were obtained from transplant donors (n=5) from Cleveland Clinic and had an average age of

23yr +/- 7yrs. All tissue homogenization and lipoprotein fractionation procedures were performed within a cold room to ensure maintaining tissue and sample temperatures under 4°C. Frozen tissue blocks (submerged in 65 mM sodium phosphate buffer, pH 7.4, under argon, within screw cap containers) were thawed by placement of the containers in ice/water bath. Immediately before complete thaw, ice-cold Ca₂⁺ and Mg₂⁺-free Chelex-100 treated PBS supplemented with 100 µM DTPA, pH 7.4 was added to rinse the tissue five times to remove any residual blood from tissue. The aorta segment was cleaned of adventitial fat and again rinsed three times with ice-cold PBS supplemented with 100 µM DTPA. Wet weigh of the aorta was determined, the tissue cut into small pieces, and then suspended in ice-cold Ca²⁺ and Mg²⁺-free PBS supplemented with both 100 µM DTPA, (pH 7.4) and a protease inhibitor cocktail (Sigma-Aldrich, catalog number P8340), which was included in all subsequent solutions used for homogenization and lipoprotein isolation. Aortic tissues were homogenized in ice/water bath with a motor-driven Brinkmann homogenizer for 30sec intervals five times with 2 minutes rest between homogenizations. Care was taken throughout homogenization to maintain a temperature at or close to 0°C by keeping the homogenization vessel submerged within slush (ice/water bath). The crude homogenate was centrifuged at low speed 15,000 ×g for 30 min at 0°C and the pellet discarded. This low speed supernatant (lesion homogenate) was then used for buoyant density isolation of LDL/VLDL (d<1.063), HDL (1.063 d 1.21) and lipoprotein-depleted (LPD) fractions (d>1.21). Fractions were dialyzed at 4°C four times against 4 liters of 5 mM ammonium bicarbonate, with 50 µM DTPA (pH 7.4) and 25 µM BHT changed every four hours. A last change of buffer was against 4 liters of ice-cold Chelex-100 treated 1× PBS, pH7.4.

Immuno-affinity isolation of apoA1 from aortic tissue homogenate—Immuno-affinity resin was generated by covalently coupling mAb 10G1.5 to AminoLink Plus (Pierce Chemical, Rockford, IL) resin at a density of 1.5 mg antibody per ml of resin in an amine-free buffer (PBS, pH 7.4) as per the manufacturer's instruction. Reactive non-antibody-bound sites on the resin were blocked with addition of excess ethanolamine. The affinity gel was drained and antibody concentration in the flow through determined in order to calculate cross-linking efficiency, which was greater than 90%. The gel was then extensively rinsed with 1M TRIS, pH 7.4, 1M NaCl, and then equilibrated in 1× PBS, pH 7.4 prior to use or storage (0.002% sodium azide was added if stored). Individual one-time use affinity columns (1 ml, drained resin) were prepared with immobilized 10G1.5, and artery wall apoA1 was purified from individual samples of aortic homogenates under conditions that quantitatively recovered apoA1, as confirmed using Western blot analyses of column fractions.

LCAT activity—Human recombinant LCAT was prepared and purified from culture medium of a CHO cell line (generously provided by John Parks, Wake Forest University, NC) with stable expression human LCAT²¹. LCAT activity was determined by calculating the conversion efficiency of [³H]cholesterol to [³H]cholesteryl ester after lipid extraction of the reaction mixture followed by thin-layer chromatography²². Fractional cholesterol esterification was calculated as dpm in cholesterol esters divided by dpm in cholesterol esters plus free cholesterol. The fractional cholesterol esterification rate was expressed as Units of activity (nanomoles of cholesterol ester formed per hour per ng of LCAT) per µg apoA1 protein.

Cholesterol efflux activity—Cholesterol efflux experiments were performed according to established procedures²³. The cholesterol efflux was calculated as the total radioactivity in the medium / (medium radioactivity plus cell radioactivity). Results are expressed as a percentage relative to cholesterol efflux measured using human apoA1 isolated from healthy donors (n=5) as control.

HDL imaging—HDL was dual-labeled and incubated with mouse peritoneal macrophages to individually monitor the fate of phospholipid versus protein components of the particle as follows. Briefly, the protein component of isolated human HDL was first labeled with Alexa Fluor 633 reactive dye kit (Molecular Probes, Eugene, OR) according to the manufacturer instructions. HDL lipid was next labeled by first forming a phospholipid film of NBD-PE by evaporation of a 1:4, methanol:chloroform solution overnight under vacuum, and then rehydrating the film with Alexa Fluor 633-labeled HDL in pre-filtered PBS and 4 cycles of alternating rounds of sonication at 0°C for 1 min, followed by a 1 min interval on ice. Dual-labeled HDL was centrifuge filtered and washed numerous times with PBS prior to incubation with macrophages. Thioglycolate-elicited peritoneal macrophages from C57Blk/6J mice were collected and cultured as described²⁴. Dual labeled HDL (125 µg protein/ml) was incubated with cells at 37°C for 1 hour, and then images were captured on a Zeiss LSM 510 Meta confocal microscope.

Proteomic analyses—To confirm the protein recovered following immuno-affinity isolation (using mAb 10G1.5) from normal aortic tissues homogenate was apoA1, the major SDS-PAGE gel bands at molecular weight 25kDa and 50kDa were excised. The samples were first treated with dithiothreitol/iodoacetamide (Sigma, St. Louis, MO) in order to carbamidomethylate any cysteines in the protein(s) and then proteins were digested using Mass Spec grade trypsin (Promega, Madison, WI) at 37°C overnight. Tryptic peptides were loaded onto an IntegraFrit sample trap (ProteoPep C18, 300 Å, 150 µm × 2.5 cm, New Objective, Woburn MA) at 1 µL/min with 5% acetonitrile and 0.1% formic acid in order to desalt the samples. The peptides were subsequently eluted through a column (75 µm × 15 cm) packed in-house with XperTek 218TP, C18, 300 Å pore size, 150 µm particle size (Cobert Associates, St. Louis, MO) at 200 nL/min using a Proxeon Easy-nLC II system (Thermo Scientific, Waltham MA) with a gradient of 5–65% acetonitrile, 0.1% formic acid over 120 minutes into a LTQ-Orbitrap Velos mass spectrometer (Thermo Scientific, Waltham MA). Peak lists were generated using Proteome Discoverer 1.1 (Thermo Fischer Scientific, Waltham, MA). The resulting Unified Search Files (*.srf) were searched against the Uniprot FASTA of all apolipoproteins and also against a human protein database downloaded from the European Bioinformatic Institute (EBI, release: 2013_02). Modifications used for searches included carbamidomethylated cysteine (fixed), oxidized methionine and tryptophan (variable), 3-chloro and 3-nitro tyrosine (variable). Only strictly tryptic peptides with a maximum of 2 missed cleavage site were allowed in the database searches. Monoisotopic precursor ions were searched with a tolerance of 100 ppm with 0.8 Da for the fragment ions on the data obtained from the hybrid LTQ-Orbitrap Velos mass spectrometer. Unidentified fragment ions in all fragmentation spectra were manually validated using Protein Prospector (University of California, San Francisco).

Statistical Analysis—Nonparametric statistical methods were used to determine statistical differences due to sampling numbers. Wilcoxon rank sum test was used for two-group comparisons and the Kruskal-Wallis test was used for multiple-group comparisons (> two groups). In cases where Kruskal-Wallis test was performed for multiple group comparisons and found to be significant ($p < 0.05$), multiple comparison procedures such as the Dunn's test was used for pairwise comparison between groups and controls. The Wilcoxon rank sum test was also used for pairwise comparison. Where indicated, the one-sample robust Hotelling T2 test was used to determine statistical significance when comparing enzymatic activity between the control group and experimental group.

RESULTS

Monoclonal antibody 10G1.5 recognizes apoA1 equally well in its lipid-free or HDL-associated, native and oxidized forms

We initially sought to accurately quantify and immuno-affinity isolate apoA1 from artery wall tissue homogenate (from both normal and atherosclerotic lesions). We reasoned this would require a sufficiently tight binding antibody that demonstrated minimal recognition bias between lipidated versus non-lipidated forms of the lipoprotein, as well as oxidized versus non-oxidatively modified forms. Examination of every commercially available antibody we could find (both monoclonal and polyclonal) showed significant bias in recognizing one form or another (typically recognition of oxidized forms preferentially, and with inadequate affinity). Figure 1a illustrates the biases observed with three characteristic commercial antibodies (two polyclonal and one mouse monoclonal antibody). Note that despite equal mass of protein loaded into adjacent lanes from native vs. oxidized apoA1, and HDL vs. oxidized HDL, the commercial antibodies show varied intensity of staining (e.g. Commercial Ab 1 shows oxHDL>ox-apoA1>>apoA1 or HDL; Commercial Ab 2 shows ox-apoA1>oxHDL>>apoA1 or HDL; and Commercial Ab 3 shows ox-apoA1 or oxHDL>>apoA1 or HDL). We therefore sought initially to develop a suitable antibody that met our strict apoA1 recognition criteria. Purified delipidated human apoA1 (isolated from plasma HDL) was injected into several *apoA1* $-/-$ mice. After screening over 5,000 hybridoma clones for their ability to recognize apoA1 forms equally well, a small number (four) met our screening program requirements. One mAb, 10G1.5, was selected based on specific activity of recognition by ELISA, immunoblot analysis, its ability to immunoprecipitate apoA1, as well as the growth characteristics of the hybridoma clone. Figure 1b illustrates mAb 10G1.5 recognizes native apoA1 and apoA1 reconstituted into HDL particles equally well. Furthermore, mAb 10G1.5 recognizes apoA1 in native vs. oxidized forms equivalently, using a wide variety of oxidation schemes (Figure 1b). We further examined the ability of mAb 10G1.5 to quantify different concentrations of purified apoA1 (lipid-poor) versus equivalent amounts of total apoA1 in either isolated human HDL (total), or the individual HDL subfractions HDL2, or HDL3 (Figure 1c). As can be seen, mAb10G1.5 displayed nearly identical ability to quantify apoA1 in its varied lipid free and lipidated forms over a range of masses. Based upon the observed unbiased recognition of all apoA1 forms, we refer to this antibody as "anti-total" apoA1. This mAb was used throughout the studies described below to detect, immuno-affinity purify and quantify apoA1 recovered from plasma, atherosclerotic lesion homogenates and normal artery wall homogenates.

The vast majority of apoA1 isolated from lesions is highly cross-linked and not HDL-associated

The particle distribution of apoA1 within human atherosclerotic lesions has not been reported. We therefore homogenized human aortic atherosclerotic lesions (n=10 different subjects) and used sequential buoyant density ultracentrifugation to initially remove the VLDL/LDL-like fraction ($d < 1.063$), and then recover both HDL-like fraction ($1.063 < d < 1.21$) and the lipoprotein-depleted (LPD) fraction (density > 1.21), as described under Methods. Samples were first examined on gradient (5–15%) SDS-polyacrylamide (SDS-PAGE) separations using Sypro Ruby Red protein staining, which shows minimal protein-to-protein differences in staining, equally stains lipoproteins, glycoproteins, and other difficult to stain proteins, and also does not interfere with subsequent mass spectrometry analyses. Visual inspection shows a complex protein mixture, with an unknown band migrating at ~27 kDa, the molecular weight of apoA1 (Figure 2a). Western analysis with anti-total apoA1 antibody (mAb 10G1.5) of a membrane containing transferred proteins from a parallel-run duplicate gel readily detected within lesion homogenates a band at the

molecular weight of the apoA1 monomer (Figure 2b). Remarkably, the vast majority of apoA1 within the aortic lesion was observed to be present not within the HDL-like fraction, but rather, within the LPD fraction (Figure 2b). After substantial increase in exposure of the immunoblot, apoA1 was detected within the HDL-like particle fraction (Figure 2c). Also notable within the immunoblots were prominent slower migrating forms of immuno-reactive apoA1-containing protein bands at molecular weights of ~50, ~75 and ~100 kDa present in particular within the starting material (homogenate) and the LPD fraction (density > 1.21), but noticeably diminished in the HDL-like particle fraction (1.063 d 1.21). The sizes of these slower migrating apoA1-immuno-reactive bands are consistent with the sizes of oxidatively cross-linked dimeric and multimeric apoA1 forms.

Quantification of the distribution of protein and apoA1 forms recovered within homogenates from multiple distinct human atherosclerotic plaque-laden aorta (n=10) is shown in Figure 3. The majority ($81.0 \pm 5.6\%$) of the total protein in the lesion homogenate was found in the LPD fraction, while the HDL-like fraction contained only $1.7 \pm 0.2\%$ (Figure 3a). Quantitative analysis of the anti-total apoA1-specific immunoblots indicated that nearly all of the apoA1 isolated from lesions was lipid-poor, and found within the LPD fraction (density > 1.21) where $0.7 \text{ mg} \pm 0.4 \text{ mg}$ apoA1 per gram wet weight of lesion material was recovered (Figure 3b), corresponding to $92.4 \pm 4.1\%$ of total apoA1 in the artery wall (Figure 3c). Surprisingly, only a nominal amount (< 3%) of apoA1 within the artery wall (lesions) was recovered in the HDL-like particle fraction (Figure 3b,c). Yet another remarkable finding is the abundance of slower migrating immuno-reactive apoA1-containing bands migrating with molecular masses of dimeric, trimeric and tetrameric forms of apoA1 within the lesion homogenates. Quantification of these apoA1-immuno-reactive bands revealed that approximately two thirds ($66 \pm 4\%$) of apoA1 within lesions is oxidatively cross-linked, and the cross-linked forms are preferentially present in the LPD fraction (Figure 3d). Proteomics analyses of anti-total apoA1 (mAb 10G1.5) immunoprecipitated higher molecular weight apoA1 forms confirmed these bands too were predominately comprised of apoA1 (see below). It should be noted that total apoA1 present in the aortic tissues reported are actually modestly underestimated as we know that under the conditions employed, approximately 15–20% of the total apoA1 remains unrecovered in the “pellet” from the initial tissue homogenate. This modest loss appeared acceptable since control studies with repeated homogenization of the pellet and fractionation of the recovered material revealed, within both crude homogenate and subsequent buoyant density isolated fractions, virtually identical banding pattern and results to the original homogenate and fractions, based upon both protein staining and Western blot analyses (data not shown).

ApoA1 is markedly enriched in lesions, and normal aortic tissue apoA1 similarly is lipid-poor and highly cross-linked

Our initial studies focused on apoA1 within atherosclerotic lesions. However, given the surprising finding that virtually all apoA1 within aortic lesions was not on an HDL particle, and fully two-thirds of all apoA1 within lesions was cross-linked, we decided to examine apoA1 within normal aortic tissue for comparison. Normal aortic tissue was obtained at time of organ harvest from transplant donors. For illustrative purposes, an image of a typical normal aortic specimen, and a typical atherosclerotic plaque-laden aortic specimen, are shown in Figure 4a. Homogenates of normal aortic tissue (n=5) were prepared and fractionated by buoyant density ultracentrifugation as described in Methods. Fractionation of protein from normal artery and lesion homogenates on (5–15%) gradient reducing SDS-PAGE gels stained with Sypro Ruby Red for protein reveal that although there are similarities in the protein banding pattern, the pattern is noticeably different in normal vs. lesion homogenates (Figure 4b). Notably, immunoblot probing with apoA1-specific anti-total apoA1 (mAb 10G1.5) of parallel SDS-PAGE gels transferred to membranes showed

that compared to lesion-derived homogenates, there is very little immune-reactive apoA1 in homogenates prepared from normal aortic tissue (Figure 4c). Since extremely low levels of apoA1 were observed within normal artery wall tissue, and especially the HDL-like fraction, an increased protein amount was loaded onto SDS-PAGE gels to permit visualization by Western and comparison of HDL-like and LPD fractions from the normal artery wall homogenate (Figure 4d). The majority of protein in the normal artery wall homogenate was found to be in the LPD fraction (Supplemental Figure 1). As observed for aortic lesion apoA1, a significant portion of apoA1 was lipid-poor and recovered within the LPD fraction. Further, there was a high degree of immuno-reactive apoA1 forms in the normal artery wall that migrate at higher molecular weights, consistent with that of oxidatively cross-linked apoA1 dimer and higher multimeric forms, particularly within the LPD fraction (Figure 4d).

Quantification of apoA1-specific immuno-blots (and taking into account volumes of starting homogenate and density cut fractions recovered) revealed that the total apoA1 recovered per gram of wet weight aortic tissue from normal artery wall was 120-fold less than that recovered from lesion-laden aorta (Figure 4e, note log scale for Y axis). Remarkably, the distribution of apoA1 within normal artery resembled those found in the same fractions from atherosclerotic lesions, with only 3% of apoA1 being HDL-associated, and approximately 92% of the total apoA1 present in the normal artery wall residing in the LPD fraction (Figure 4f). Similar to that observed within lesions, nearly half ($43.4 \pm 13.9\%$) of the total apoA1 within the normal artery wall was cross-linked and observed to reside not on the HDL-like particle ($3.6 \pm 2.6\%$), but in the LPD fraction ($61.4 \pm 23.0\%$; Figure 4g).

Since the levels of apoA1 in the normal artery wall-derived homogenates were so low, we wanted to verify that the bands detected on Westerns using mAb 10G1.5 were in fact apoA1. We therefore immuno-purified apoA1 from normal aortic tissue homogenates ($n=5$) using 10G1.5 (as described in Methods), and immuno-affinity isolated proteins were separated on a gradient non-reducing (5–15%) SDS-PAGE gel and stained for protein. The major protein bands observed corresponded to doublet bands migrating at ~ 25 kDa and ~ 50 kDa (Supplemental Figure 2). These were individually excised and digested with trypsin for mass spectrometry analyses as described in Methods. Tandem MS analyses of tryptic peptides for each excised band revealed apoA1 as the dominant protein within each, with 40–62% peptide coverage in each of the gel-excised bands (Supplemental Tables 1–4).

Plasma apoA1 is predominantly HDL-associated, and has decreased apoA1 cross-links in the HDL-like fraction compared to the LPD fraction

Given the surprising HDL particle distribution and cross-link prevalence of apoA1 found in the artery wall (Figures 2–4), and the known preponderance of apoA1 within the HDL fraction in plasma, we examined the distribution of apoA1 in plasma using the same anti-total apoA1 mAb (10G1.5). Plasma from normal healthy consenting donors was fractionated by sequential buoyant density ultracentrifugation as described in Methods. The indicated amount of protein from the starting material plasma, HDL-rich fraction and lipoprotein depleted fractions were run on gradient (5–15%) reducing SDS-PAGE gels and stained with Coomassie Blue (Figure 5a), or transferred for immunoblot analyses with anti-apoA1 mAb 10G1.5 (Figure 5b). As expected, the dominant immuno-reactive band observed migrates at ~ 27 kDa, corresponding to the apoA1 monomer, and is predominantly recovered within the HDL fraction ($\sim 83\%$; Figure 5b,d). Unlike apoA1 recovered from the artery wall, there is little noticeable higher molecular weight cross-linked apoA1 in the starting plasma, particularly within the circulating HDL fraction. Of note, however, the content of apoA1 cross-linked within the LPD fraction was found to be 3-fold higher than that observed within the HDL fraction, but still represented only a small minority ($6.0 \pm 1.8\%$) of the total apoA1 within that fraction (Figure 5e, and longer exposure of plasma and LPD fractions are shown in Supplemental Figure 3).

ApoA1 isolated from atherosclerotic lesions is dysfunctional—In a final series of experiments, apoA1 was isolated from additional atherosclerotic plaque-laden aortic tissues (n=10 subjects) by individual immuno-affinity columns comprised of immobilized anti-total apoA1 (mAb 10G1.5), as described under Methods. Immuno-isolated apoA1 was quantified and equivalent amounts of apoA1 protein recovered from lesions from each sample, or apoA1 purified from plasma HDL (as a control) were incubated with cholesterol-loaded murine macrophage RAW264.7 cells to quantify cholesterol efflux activity. Remarkably, every apoA1 sample recovered from plaque-laden aorta demonstrated lower cholesterol acceptor activity, showing $78.9\% \pm 6.0\%$ less total cholesterol efflux capacity compared to control apoA1 purified from plasma HDL from healthy donors (Figure 6). In parallel studies, each of the lesion apoA1 were incorporated into reconstituted HDL by cholate dialysis method, further purified by gel filtration FPLC, and then comparable amounts (5 μ g apoA1 mass) of each rHDL was examined for LCAT activity and compared with rHDL generated from apoA1 purified from plasma HDL from healthy volunteers. rHDL formed with lesion apoA1 demonstrated significantly less ($89.6\% \pm 5.0\%$) LCAT activity compared to rHDL formed from control apoA1 (Figure 6). Thus, apoA1 in atherosclerotic plaque-laden aorta is markedly functionally impaired (i.e. “dysfunctional”) with respect to both cholesterol acceptor and LCAT activities.

DISCUSSION

The present studies reveal multiple remarkable findings about apoA1 within the artery wall. First, the vast majority of apoA1 within both normal and atherosclerotic human arterial tissue, in contrast to within the circulation, is lipid-poor (i.e., in the LPD fraction, $d > 1.21$), and does not reside on an HDL-like ($1.063 < d < 1.21$) particle. Second, the content of apoA1 in atherosclerotic lesions is over 100-fold higher than that observed within normal artery wall. Third, the majority of apoA1 within arterial tissues (both normal and atherosclerotic) is oxidatively cross-linked. Fourth, apoA1 within arterial tissues is “dysfunctional”, with ~80% reduction in cholesterol acceptor activity and ~90% reduction in capacity to activate LCAT. Fifth, the majority of oxidatively cross-linked apoA1 within the circulation is not HDL particle associated, but rather, resides within the lipoprotein-depleted fraction ($d > 1.21$). Collectively, the present studies thus argue that examination of total apoA1 and HDL function within the circulation may not adequately represent what is occurring within the artery wall, especially with respect to cholesterol acceptor and LCAT activities. Moreover, the overall strategy applied in the present studies may prove useful when examining other post-translational modifications to apoA1, such as glycation, and site-specific oxidative modifications, as antibodies become available. Finally, the present studies suggest that the common practice of isolating circulating HDL for study of its biological properties, and discarding the lipid-poor (non-HDL associated) apoA1, may in fact be throwing out the very fraction (lipid-poor) that more closely reflects the environment within the artery wall. Of note, the extent of oxidatively cross-linked apoA1 within the lipid-poor (lipoprotein-depleted) fraction of plasma was approximately 3-fold enriched relative to the HDL-like fraction (Figure 5e). Based upon the cumulative results herein one might speculate that “dysfunctional” forms of HDL monitored within the circulation will most likely reside not on the HDL particle itself, but as lipid-poor forms in the LPD fraction ($d > 1.21$). It is notable that the apoA1 found within the artery wall, which was predominantly within the LPD fraction in both atherosclerotic lesions and normal artery wall tissue, is remarkably highly cross-linked (50–70%). This value is even higher than previously observed in Western blots (though cross-linking was not quantified per se) in studies examining apoA1 oxidation levels in the artery wall based upon buoyant density recovery of HDL-like particles⁸. Through use of stable isotope dilution mass spectrometry based approaches, these studies suggested an upper boundary of up to one of every two HDL-like particles recovered

from the artery wall carried an oxidative modification from either MPO- or NO-derived oxidants⁸.

One question the current studies raise is how apoA1 becomes over 100-fold enriched within atherosclerotic plaques compared to normal artery. A second question is how artery wall apoA1 is rendered lipid-poor, when the vast majority of apoA1 that diffuses into the artery wall tissue from the circulation resides within the HDL particle. To address these questions we performed preliminary confocal microscopy studies where HDL was isolated from peripheral blood of healthy volunteers and subsequently doubly labeled (protein with AF 633 (red), and phospholipid with NBD-PE (green) as described in Methods). Brief incubation of the doubly-labeled HDL with macrophages led to virtually all of the phospholipid fluorophore being rapidly taken up within the macrophage, whereas the protein (predominantly apoA1) remained on the cell surface (data not shown). Such preliminary results provide rationale to speculate that selective uptake of lipids may contribute as a mechanism for rapidly depleting the HDL particle of not just cholesterol but also phospholipid, leaving the lipid-poor apoA1 behind in the extracellular space. Lipid-poor or lipid-free forms of apoA1 are recognized as the preferred substrate of ABCA1^{5, 25-27}. So a question that logically follows is why the lipid-poor apoA1 form within the artery wall is such a poor cholesterol acceptor (Figure 6). In past studies we have shown that oxidative modification of apoA1 by MPO-generated oxidants markedly impairs its ABCA1-dependent cholesterol efflux activity^{8-10, 13}. Other studies have also reported that carboxy-terminal proteolyzed (ie "clipped") apoA1 can be recovered from aortic tissue that fails to efficiently bind lipid^{28, 29}. In the present studies, however, we did not see substantial levels of lower molecular weight forms of apoA1 in tissue homogenates once we exercised extreme care in keeping tissues ice-cold, and more importantly, included an extensive cocktail of protease inhibitors during tissue dissection, homogenization and fractionation as outlined under Methods. Given the extensive oxidative cross-linking observed in total apoA1 within lesions, oxidative post-translational modifications of apoA1 likely explain in large part why the lipoprotein, at least within lesions, remains lipid-poor. It should also be noted, however, that Parks and colleagues reported that interaction of apoA1 with ABCA1 results in lipid-poor "pre-beta HDL" migrating forms of apoA1 that themselves are poor substrates for subsequent repeat or further lipidation by ABCA1, suggesting the requirement of an additional (non-ABCA1-mediated) process for further maturation into an HDL particle²⁶. Whether this contributes to the current results is unclear. Similarly, if an additional process is needed for further lipidation of lipid-poor apoA1 after initial interaction with ABCA1, whether this process is somehow lacking or inhibited within the artery wall requires further study. It also would have been interesting to test if reconstituted HDL made with apoA1 isolated from the vessel wall was also defective in either ABCG1 or passive efflux compared to HDL made with plasma derived apoA1. However, given the limitations in the amount of apoA1 able to be purified from human arterial tissues, these studies will need to await further investigation.

As for the mechanism(s) for apoA1 accumulation within lesions compared to normal artery, we have no clear answers from the present studies. We can speculate that the extensive oxidative cross-linking noted here, and through mass spectrometry studies in the past^{8-10, 13}, may help provide an answer. Oxidatively modified proteins tend to be less soluble, relatively protease resistant, and might thus be "retained" within the subendothelial space, particularly within the hydrophobic environment of the atherosclerotic plaque. The phenomenon of lipoprotein retention within the subendothelial compartment of the artery wall has previously been suggested. Originally proposed for apoB-lipoproteins, retention or trapping of LDL particles in the initial stages of atherosclerosis is suggested to cultivate formation of modified LDL, which may incite biological and inflammatory responses that initiate or progress the atherosclerotic process³⁰. Progressive apoB lipoprotein retention through the

actions of secretory acid sphingomyelinase and lipoprotein lipase are thought to lead to accelerated lesion progression^{31, 32}. While we have no data to implicate lipase activation at present in depleting lipids from HDL within the artery wall leading to lipid-depleted forms, the presence of similar phospholipids on HDL suggests a similar retention scheme for apoA1 lipoprotein retention is feasible, and could thus contribute to the observed accumulation of apoA1 in artery wall lesions over time, in addition to enhanced lipid and sterol uptake into macrophages producing foam cells. Other studies have also shown that there is increased endothelial cell permeability in atherosclerotic lesions which could lead to increased LDL and HDL migration into the diseased vessel wall and accelerate the retention process³³⁻³⁵.

While multiple studies have noted extensive oxidative modification of apoA1 recovered from the artery wall^{8-11, 13-16, 36}, it should be noted that there has been disagreement as to which residues are the main sites of oxidation. Of note, our prior proteomic mapping studies employed polyclonal antibodies (chicken anti-apoA1 or anti-HDL) to immuno-precipitate apoA1 from arterial tissue homogenates^{13, 16}. In contrast, proteomic mapping studies from alternative groups typically have used buoyant density isolation to recover the HDL-like particle fraction within lesion homogenates^{11, 15}. Based on the present studies using the mAb 10G1.5, which was developed specifically to allow both recovery and equal quantification of apoA1 in lipid-free vs. lipidated, and native vs. oxidized forms, it is now clear that analysis of recovered HDL-like particles from arterial tissues only examines a very small fraction (<3%) of the total apoA1 within the artery wall. Whether the small amount of apoA1 (and its associated proteome) recovered in an HDL-like particle from the artery wall provides a "snapshot" of the apoA1 on its way to particle "disintegration" and formation of the lipid-poor apoA1 that is the predominant form remains to be determined. The present studies suggest that results which focus on HDL-like particles recovered from the artery wall need to be interpreted within the context of recognizing their minor quantitative contribution to total apoA1 in the artery wall. An interesting question, though not examined in the present studies, is whether changes in the HDL-associated proteome within the circulation observed in subjects with cardiovascular disease, or within subjects at heightened risk for cardiovascular disease³⁷⁻⁴¹, have any relevance to the marked changes in the environment of apoA1 observed within the artery wall.

The complexity surrounding the role of the HDL particle in the pathogenesis of cardiovascular disease has been highlighted recently because of several high profile clinical trial failures targeting raising of HDL cholesterol, and recent Mendelian randomization studies on HDL cholesterol levels^{1, 2, 4, 42-47}. The present studies suggest that traditional HDL measured parameters within the circulation, such as HDL cholesterol, and apoA1 mass, may not adequately reflect the biology of apoA1 occurring within the artery wall. Recent studies suggest that functional measures of cholesterol efflux activity within apolipoprotein B-depleted serum may serve as a superior surrogate for HDL function⁴⁸. However, this too has recently been questioned because the HDL particle was found to only account for a minority of the cholesterol acceptor activity in the cholesterol efflux activity assays performed⁴⁹. Further, despite the reported inverse association between cholesterol efflux activity and prevalent cardiovascular disease, in a separate large clinical study of similar patients (i.e. sequential subjects undergoing elective diagnostic coronary angiography), enhanced cholesterol efflux activity was observed to paradoxically associate with increased prospective cardiovascular event risk⁴⁹. It is remarkable that what we now recognize as HDL was first described nearly a century ago⁵⁰. And yet, studies focusing on HDL still continue to surprise, and reveal how little we know about its complex biology. The present and recent studies suggest that measurement in the circulation of HDL cholesterol, apoA1, or even cholesterol efflux activity, may not adequately reflect what is happening within the artery wall. Rather, development of "dysfunctional HDL" assays that

detect structurally specific modified forms of apoA1 formed in the artery wall but which diffuse back out into the circulation may be what is needed to provide insights into the processes happening within the artery wall.

Supplementary Material

Refer to Web version on PubMed Central for supplementary material.

Acknowledgments

Funding Sources: This study was supported by National Institutes of Health grants P01HL098055, P01HL076491, and HL17964. This work was also supported in part by a grant from the LeDucq Foundation. Dr. Hazen was also partially supported from a gift of the Leonard Krieger Foundation.

Dr. Tang has previously received research grant support from Abbott Laboratories. Drs. Hazen and Smith report being listed as co-inventor on pending and issued patents held by the Cleveland Clinic relating to cardiovascular diagnostics. Dr. Hazen reports having been paid as a consultant for the following companies: AstraZeneca Pharmaceuticals LP, Cleveland Heart Lab, Esperion, Lilly, Liposcience Inc., Merck & Co., Inc., Pfizer Inc., and Takeda. Dr. Hazen reports receiving research funds from Abbott, Cleveland Heart Lab, and Liposcience Inc. Dr. Smith reports having the right to receive royalty payments for inventions or discoveries related to cardiovascular diagnostics from Cleveland Heart Lab and being paid as a consultant for Esperion. Dr. Hazen reports having the right to receive royalty payments for inventions or discoveries related to cardiovascular diagnostics and the companies shown below: Cleveland Heart Lab., Frantz Biomarkers, LLC, Liposcience Inc., and Siemens.

References

1. Barter PJ, Caulfield M, Eriksson M, Grundy SM, Kastelein JJ, Komajda M, Lopez-Sendon J, Mosca L, Tardif JC, Waters DD, Shear CL, Revkin JH, Buhr KA, Fisher MR, Tall AR, Brewer B. Effects of torcetrapib in patients at high risk for coronary events. *N Engl J Med.* 2007; 357:2109–2122. [PubMed: 17984165]
2. Boden WE, Probstfield JL, Anderson T, Chaitman BR, Desvignes-Nickens P, Koprowicz K, McBride R, Teo K, Weintraub W. Niacin in patients with low hdl cholesterol levels receiving intensive statin therapy. *N Engl J Med.* 2011; 365:2255–2267. [PubMed: 22085343]
3. Schwartz GG, Olsson AG, Abt M, Ballantyne CM, Barter PJ, Brumm J, Chaitman BR, Holme IM, Kallend D, Leiter LA, Leitersdorf E, McMurray JJ, Mundl H, Nicholls SJ, Shah PK, Tardif JC, Wright RS. Effects of dalcetrapib in patients with a recent acute coronary syndrome. *N Engl J Med.* 2012; 367:2089–2099. [PubMed: 23126252]
4. Voight BF, Peloso GM, Orho-Melander M, Frikke-Schmidt R, Barbalic M, Jensen MK, Hindy G, Holm H, Ding EL, Johnson T, Schunkert H, Samani NJ, Clarke R, Hopewell JC, Thompson JF, Li M, Thorleifsson G, Newton-Cheh C, Musunuru K, Pirruccello JP, Saleheen D, Chen L, Stewart A, Schillert A, Thorsteinsdottir U, Thorgeirsson G, Anand S, Engert JC, Morgan T, Spertus J, Stoll M, Berger K, Martinelli N, Girelli D, McKeown PP, Patterson CC, Epstein SE, Devaney J, Burnett MS, Mooser V, Ripatti S, Surakka I, Nieminen MS, Sinisalo J, Lokki ML, Perola M, Havulinna A, de Faire U, Gigante B, Ingelsson E, Zeller T, Wild P, de Bakker PI, Klungel OH, Maitland-van der Zee AH, Peters BJ, de Boer A, Grobbee DE, Kamphuisen PW, Deneer VH, Elbers CC, Onland-Moret NC, Hofker MH, Wijmenga C, Verschuren WM, Boer JM, van der Schouw YT, Rasheed A, Frossard P, Demissie S, Willer C, Do R, Ordovas JM, Abecasis GR, Boehnke M, Mohlke KL, Daly MJ, Guiducci C, Burt NP, Surti A, Gonzalez E, Purcell S, Gabriel S, Marrugat J, Peden J, Erdmann J, Diemert P, Willenborg C, König IR, Fischer M, Hengstenberg C, Ziegler A, Buyschaert I, Lambrechts D, Van de Werf F, Fox KA, El Mokhtari NE, Rubin D, Schrezenmeier J, Schreiber S, Schafer A, Danesh J, Blankenberg S, Roberts R, McPherson R, Watkins H, Hall AS, Overvad K, Rimm E, Boerwinkle E, Tybjaerg-Hansen A, Cupples LA, Reilly MP, Melander O, Mannucci PM, Ardisino D, Siscovick D, Elosua R, Stefansson K, O'Donnell CJ, Salomaa V, Rader DJ, Peltonen L, Schwartz SM, Altschuler D, Kathiresan S. Plasma hdl cholesterol and risk of myocardial infarction: A mendelian randomisation study. *Lancet.* 2012; 380:572–580. [PubMed: 22607825]
5. Rye KA, Barter PJ. Formation and metabolism of pre-beta-migrating, lipid-poor apolipoprotein a-i. *Arterioscler Thromb Vasc Biol.* 2004; 24:421–428. [PubMed: 14592845]

6. Chao FF, Amende LM, Blanchette-Mackie EJ, Skarlatos SI, Gamble W, Resau JH, Mergner WT, Kruth HS. Unesterified cholesterol-rich lipid particles in atherosclerotic lesions of human and rabbit aortas. *Am J Pathol.* 1988; 131:73–83. [PubMed: 3354646]
7. Tirziu D, Dobrian A, Tasca C, Simionescu M, Simionescu N. Intimal thickenings of human aorta contain modified reassembled lipoproteins. *Atherosclerosis.* 1995; 112:101–114. [PubMed: 7772061]
8. Zheng L, Nukuna B, Brennan ML, Sun M, Goormastic M, Settle M, Schmitt D, Fu X, Thomson L, Fox PL, Ischiropoulos H, Smith JD, Kinter M, Hazen SL. Apolipoprotein a-i is a selective target for myeloperoxidase-catalyzed oxidation and functional impairment in subjects with cardiovascular disease. *J Clin Invest.* 2004; 114:529–541. [PubMed: 15314690]
9. Wu Z, Wagner MA, Zheng L, Parks JS, Shy JM 3rd, Smith JD, Gogonea V, Hazen SL. The refined structure of nascent hdl reveals a key functional domain for particle maturation and dysfunction. *Nat Struct Mol Biol.* 2007; 14:861–868. [PubMed: 17676061]
10. Undurti A, Huang Y, Lupica JA, Smith JD, DiDonato JA, Hazen SL. Modification of high density lipoprotein by myeloperoxidase generates a pro-inflammatory particle. *J Biol Chem.* 2009; 284:30825–30835. [PubMed: 19726691]
11. Pennathur S, Bergt C, Shao B, Byun J, Kassim SY, Singh P, Green PS, McDonald TO, Brunzell J, Chait A, Oram JF, O'Brien K, Geary RL, Heinecke JW. Human atherosclerotic intima and blood of patients with established coronary artery disease contain high density lipoprotein damaged by reactive nitrogen species. *J Biol Chem.* 2004; 279:42977–42983. [PubMed: 15292228]
12. Hadfield KA, Pattison DI, Brown BE, Hou L, Rye KA, Davies MJ, Hawkins CL. Myeloperoxidase-derived oxidants modify apolipoprotein a-i and generate dysfunctional high-density lipoproteins: Comparison of hypothiocyanous acid (hosc⁻) with hypochlorous acid (hoCl). *Biochem J.* 2013; 449:531–542. [PubMed: 23088652]
13. Zheng L, Settle M, Brubaker G, Schmitt D, Hazen SL, Smith JD, Kinter M. Localization of nitration and chlorination sites on apolipoprotein a-i catalyzed by myeloperoxidase in human atheroma and associated oxidative impairment in abca1-dependent cholesterol efflux from macrophages. *J Biol Chem.* 2005; 280:38–47. [PubMed: 15498770]
14. Peng DQ, Wu Z, Brubaker G, Zheng L, Settle M, Gross E, Kinter M, Hazen SL, Smith JD. Tyrosine modification is not required for myeloperoxidase-induced loss of apolipoprotein a-i functional activities. *J Biol Chem.* 2005; 280:33775–33784. [PubMed: 16091367]
15. Shao B, Bergt C, Fu X, Green P, Voss JC, Oda MN, Oram JF, Heinecke JW. Tyrosine 192 in apolipoprotein a-i is the major site of nitration and chlorination by myeloperoxidase, but only chlorination markedly impairs abca1-dependent cholesterol transport. *J Biol Chem.* 2005; 280:5983–5993. [PubMed: 15574409]
16. Peng DQ, Brubaker G, Wu Z, Zheng L, Willard B, Kinter M, Hazen SL, Smith JD. Apolipoprotein a-i tryptophan substitution leads to resistance to myeloperoxidase-mediated loss of function. *Arterioscler Thromb Vasc Biol.* 2008; 28:2063–2070. [PubMed: 18688016]
17. Stahlman M, Davidsson P, Kanmert I, Rosengren B, Boren J, Fagerberg B, Camejo G. Proteomics and lipids of lipoproteins isolated at low salt concentrations in d₂o/sucrose or in kbr. *J Lipid Res.* 2008; 49:481–490. [PubMed: 18025001]
18. Wu Z, Gogonea V, Lee X, Wagner MA, Li XM, Huang Y, Undurti A, May RP, Haertlein M, Moulin M, Gutsche I, Zaccari G, DiDonato JA, Hazen SL. Double superhelix model of high density lipoprotein. *J Biol Chem.* 2009; 284:36605–36619. [PubMed: 19812036]
19. Matz CE, Jonas A. Micellar complexes of human apolipoprotein a-i with phosphatidylcholines and cholesterol prepared from cholate-lipid dispersions. *J Biol Chem.* 1982; 257:4535–4540. [PubMed: 6802835]
20. Nelson DP, Kiesow LA. Enthalpy of decomposition of hydrogen peroxide by catalase at 25 degrees c (with molar extinction coefficients of h₂o₂ solutions in the uv). *Anal Biochem.* 1972; 49:474–478. [PubMed: 5082943]
21. Chisholm JW, Gebre AK, Parks JS. Characterization of c-terminal histidine-tagged human recombinant lecithin:Cholesterol acyltransferase. *J Lipid Res.* 1999; 40:1512–1519. [PubMed: 10428989]

22. Parks JS, Gebre AK, Furbee JW. Lecithin-cholesterol acyltransferase. Assay of cholesterol esterification and phospholipase a2 activities. *Methods Mol Biol.* 1999; 109:123–131. [PubMed: 9918017]
23. Smith JD, Le Goff W, Settle M, Brubaker G, Waelde C, Horwitz A, Oda MN. Abca1 mediates concurrent cholesterol and phospholipid efflux to apolipoprotein a-i. *J Lipid Res.* 2004; 45:635–644. [PubMed: 14703508]
24. Piao ZH, Kim MS, Jeong M, Yun S, Lee SH, Sun HN, Song HY, Suh HW, Jung H, Yoon SR, Kim TD, Lee YH, Choi I. Vdup1 exacerbates bacteremic shock in mice infected with pseudomonas aeruginosa. *Cell Immunol.* 2012; 280:1–9. [PubMed: 23246829]
25. Wang N, Silver DL, Costet P, Tall AR. Specific binding of apo-a-i, enhanced cholesterol efflux, and altered plasma membrane morphology in cells expressing abc1. *J Biol Chem.* 2000; 275:33053–33058. [PubMed: 10918065]
26. Mulya A, Lee JY, Gebre AK, Thomas MJ, Colvin PL, Parks JS. Minimal lipidation of pre-beta hdl by abca1 results in reduced ability to interact with abca1. *Arterioscler Thromb Vasc Biol.* 2007; 27:1828–1836. [PubMed: 17510466]
27. Duong PT, Weibel GL, Lund-Katz S, Rothblat GH, Phillips MC. Characterization and properties of pre beta-hdl particles formed by abca1-mediated cellular lipid efflux to apo-a-i. *J Lipid Res.* 2008; 49:1006–1014. [PubMed: 18252847]
28. Liu L, Bortnick AE, Nickel M, Dhanasekaran P, Subbaiah PV, Lund-Katz S, Rothblat GH, Phillips MC. Effects of apolipoprotein a-i on atp-binding cassette transporter a1-mediated efflux of macrophage phospholipid and cholesterol: Formation of nascent high density lipoprotein particles. *J Biol Chem.* 2003; 278:42976–42984. [PubMed: 12928428]
29. Eriksson M, Schonland S, Yumlu S, Hegenbart U, von Hutten H, Gioeva Z, Lohse P, Buttner J, Schmidt H, Rocken C. Hereditary apolipoprotein ai-associated amyloidosis in surgical pathology specimens: Identification of three novel mutations in the apoai gene. *J Mol Diagn.* 2009; 11:257–262. [PubMed: 19324996]
30. Tabas I, Williams KJ, Boren J. Subendothelial lipoprotein retention as the initiating process in atherosclerosis: Update and therapeutic implications. *Circulation.* 2007; 116:1832–1844. [PubMed: 17938300]
31. Gustafsson M, Levin M, Skalen K, Perman J, Friden V, Jirholt P, Olofsson SO, Fazio S, Linton MF, Semenkovich CF, Olivecrona G, Boren J. Retention of low-density lipoprotein in atherosclerotic lesions of the mouse: Evidence for a role of lipoprotein lipase. *Circ Res.* 2007; 101:777–783. [PubMed: 17761930]
32. Devlin CM, Leventhal AR, Kuriakose G, Schuchman EH, Williams KJ, Tabas I. Acid sphingomyelinase promotes lipoprotein retention within early atheromata and accelerates lesion progression. *Arterioscler Thromb Vasc Biol.* 2008; 28:1723–1730. [PubMed: 18669882]
33. Vasile E, Antohe F, Simionescu M, Simionescu N. Transport pathways of beta-vldl by aortic endothelium of normal and hypercholesterolemic rabbits. *Atherosclerosis.* 1989; 75:195–210. [PubMed: 2712864]
34. Truskey GA, Roberts WL, Herrmann RA, Malinauskas RA. Measurement of endothelial permeability to 125i-low density lipoproteins in rabbit arteries by use of en face preparations. *Circ Res.* 1992; 71:883–897. [PubMed: 1516161]
35. Rozenberg I, Sluka SH, Rohrer L, Hofmann J, Becher B, Akhmedov A, Soliz J, Mocharla P, Boren J, Johansen P, Steffel J, Watanabe T, Luscher TF, Tanner FC. Histamine h1 receptor promotes atherosclerotic lesion formation by increasing vascular permeability for low-density lipoproteins. *Arterioscler Thromb Vasc Biol.* 2010; 30:923–930. [PubMed: 20203300]
36. Shao B, Pennathur S, Heinecke JW. Myeloperoxidase targets apolipoprotein a-i, the major high density lipoprotein protein, for site-specific oxidation in human atherosclerotic lesions. *J Biol Chem.* 2012; 287:6375–6386. [PubMed: 22219194]
37. Vaisar T, Pennathur S, Green PS, Gharib SA, Hoofnagle AN, Cheung MC, Byun J, Vuletic S, Kassim S, Singh P, Chea H, Knopp RH, Brunzell J, Geary R, Chait A, Zhao XQ, Elkon K, Marcovina S, Ridker P, Oram JF, Heinecke JW. Shotgun proteomics implicates protease inhibition and complement activation in the antiinflammatory properties of hdl. *J Clin Invest.* 2007; 117:746–756. [PubMed: 17332893]

38. Davidson WS, Silva RA, Chantepie S, Lagor WR, Chapman MJ, Kontush A. Proteomic analysis of defined hdl subpopulations reveals particle-specific protein clusters: Relevance to antioxidative function. *Arterioscler Thromb Vasc Biol.* 2009; 29:870–876. [PubMed: 19325143]
39. Holzer M, Wolf P, Curcic S, Birner-Gruenberger R, Weger W, Inzinger M, El-Gamal D, Wadsack C, Heinemann A, Marsche G. Psoriasis alters hdl composition and cholesterol efflux capacity. *J Lipid Res.* 2012; 53:1618–1624. [PubMed: 22649206]
40. Tolle M, Huang T, Schuchardt M, Jankowski V, Prufer N, Jankowski J, Tietge UJ, Zidek W, van der Giet M. High-density lipoprotein loses its anti-inflammatory capacity by accumulation of pro-inflammatory-serum amyloid a. *Cardiovasc Res.* 2012; 94:154–162. [PubMed: 22328092]
41. Riwanto M, Rohrer L, Roschitzki B, Besler C, Mocharla P, Mueller M, Perisa D, Heinrich K, Altwegg L, von Eckardstein A, Luscher TF, Landmesser U. Altered activation of endothelial anti- and proapoptotic pathways by high-density lipoprotein from patients with coronary artery disease: Role of high-density lipoprotein-proteome remodeling. *Circulation.* 2013; 127:891–904. [PubMed: 23349247]
42. Taylor AJ, Sullenberger LE, Lee HJ, Lee JK, Grace KA. Arterial biology for the investigation of the treatment effects of reducing cholesterol (arbiter) 2: A double-blind, placebo-controlled study of extended-release niacin on atherosclerosis progression in secondary prevention patients treated with statins. *Circulation.* 2004; 110:3512–3517. [PubMed: 15537681]
43. Vogt A, Kassner U, Hostalek U, Peiter A, Steinhagen-Thiessen E. [safety and tolerability of nicotinic acid. Results of the multicenter, open, prospective nautilus study]. *MMW Fortschr Med.* 2006; 148:41. [PubMed: 16736688]
44. Schwartz GG, Olsson AG, Ballantyne CM, Barter PJ, Holme IM, Kallend D, Leiter LA, Leitersdorf E, McMurray JJ, Shah PK, Tardif JC, Chaitman BR, Duttlinger-Maddux R, Mathieson J. Rationale and design of the dal-outcomes trial: Efficacy and safety of dalcetrapib in patients with recent acute coronary syndrome. *Am Heart J.* 2009; 158:896–901. e893. [PubMed: 19958854]
45. McKenney J, Bays H, Koren M, Ballantyne CM, Paolini JF, Mitchel Y, Betteridge A, Kuznetsova O, Sapre A, Sisk CM, Maccubbin D. Safety of extended-release niacin/laropiprant in patients with dyslipidemia. *J Clin Lipidol.* 2010; 4:105–112. e101. [PubMed: 21122637]
46. Nicholls SJ. Is niacin ineffective? Or did aim-high miss its target? *Cleve Clin J Med.* 2012; 79:38–43. [PubMed: 22219232]
47. Rader DJ, Tall AR. The not-so-simple hdl story: Is it time to revise the hdl cholesterol hypothesis? *Nat Med.* 2012; 18:1344–1346. [PubMed: 22961164]
48. Khera AV, Cuchel M, de la Llera-Moya M, Rodrigues A, Burke MF, Jafri K, French BC, Phillips JA, Mucksavage ML, Wilensky RL, Mohler ER, Rothblat GH, Rader DJ. Cholesterol efflux capacity, high-density lipoprotein function, and atherosclerosis. *N Engl J Med.* 2011; 364:127–135. [PubMed: 21226578]
49. Li X, Tang WH, Mosier MK, Huang Y, Wu Y, Matter W, Gao V, Schmitt D, DiDonato JA, Fisher EA, Smith JD, Hazen SL. Paradoxical association of enhanced cholesterol efflux with increased incident cardiovascular risks. *Arterioscler Thromb Vasc Biol.* 2013; 33:1696–1705. [PubMed: 23520163]
50. Macheboeuf M. Recherches sur les phosphoaminolipides et les sterids du serum et du plasma sanguins. Ii etude physiochimique de la fraction proteidique la plus riche en phospholipids et in sterides. Proteidique la plus riche en phospholipids et in steridesproteidique la plus riche en phospholipids et in sterides. *Bull. Soc. Chim. Biol.* 1929; 11:485–50351.

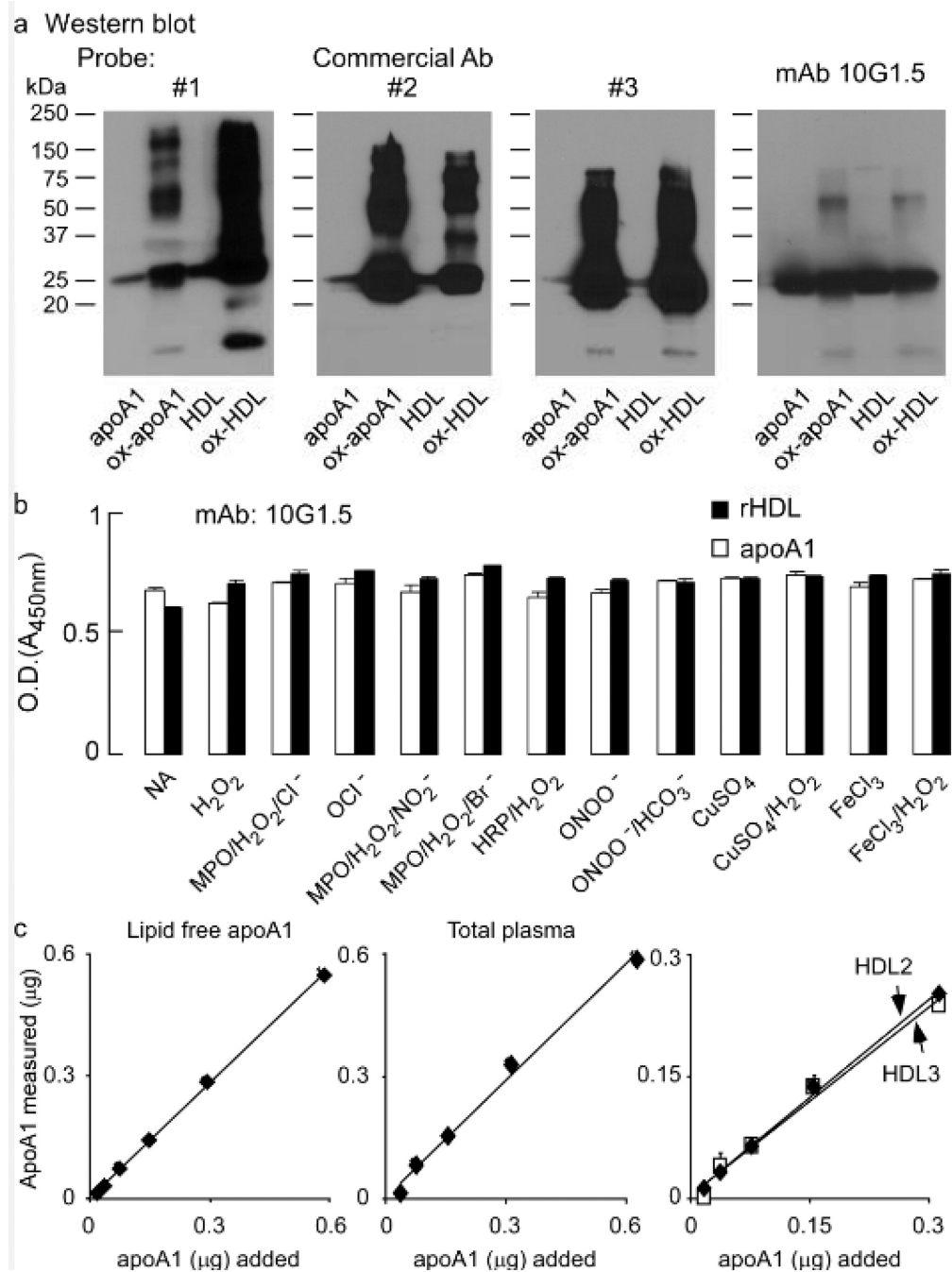


Figure 1.

ApoA1 or apoA1 in reconstituted HDL were either left untreated or oxidized at a 5:1 molar ratio of oxidant to apoA1 as described in Methods. **a**, Equal amounts of apoA1 were separated on 5–15% reducing SDS-PAGE gels and proteins transferred to membranes for Western blot detection using three distinct commercial antibodies (Ab), as indicated, or the monoclonal (mAb) 10G1.5. Monomeric and multimeric apoA1 immuno-reactive bands are apparent and Molecular weight markers are indicated. **b**, Demonstration that apoA1-specific monoclonal antibody 10G1.5 recognizes all forms of apoA1 (lipid-free and HDL-associated, non-oxidized and oxidized) equally well. ApoA1 (open bars) or reconstituted HDL (rHDL,

filled bars) prepared from apoA1 or their oxidized versions using the oxidation systems as indicated were coated at 0.5 $\mu\text{g}/\text{ml}$ into ELISA plates in triplicate and probed with 10 ng/mL anti-apoA1 monoclonal antibody 10G1.5. ELISA assays were performed as described in Methods. Reactions were stopped with 0.1N HCl, and absorbance at 450nm was determined. **c.** Lipid-free apoA1, isolated human plasma HDL, or the sub-HDL populations HDL2 and HDL3 were each loaded (in triplicate for each data point) onto 5–15% reducing SDS-PAGE gels at the indicated amounts, and then apoA1 was quantified by immuno-blot using mAb 10G1.5 as described in Methods. All values represent the average of triplicate determinations; error bars indicate the standard deviation.

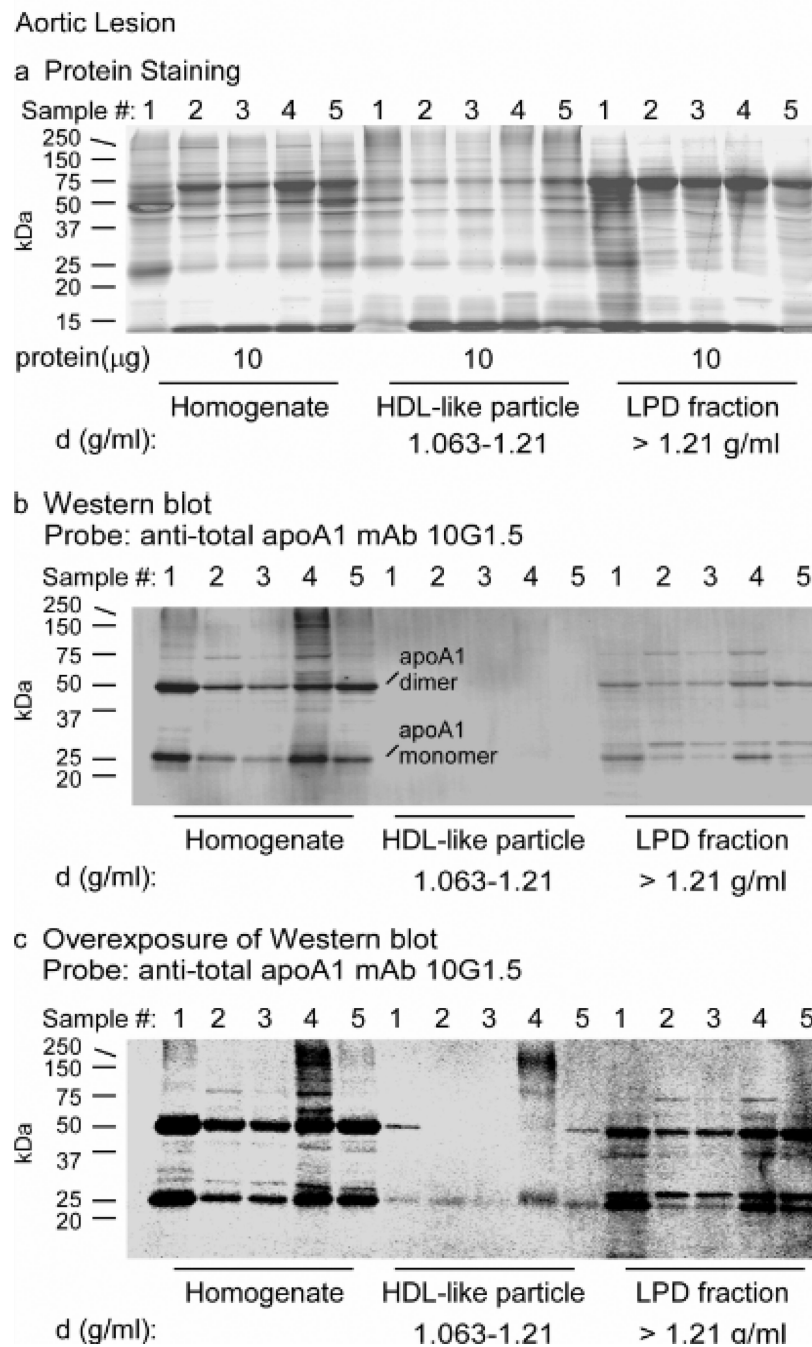
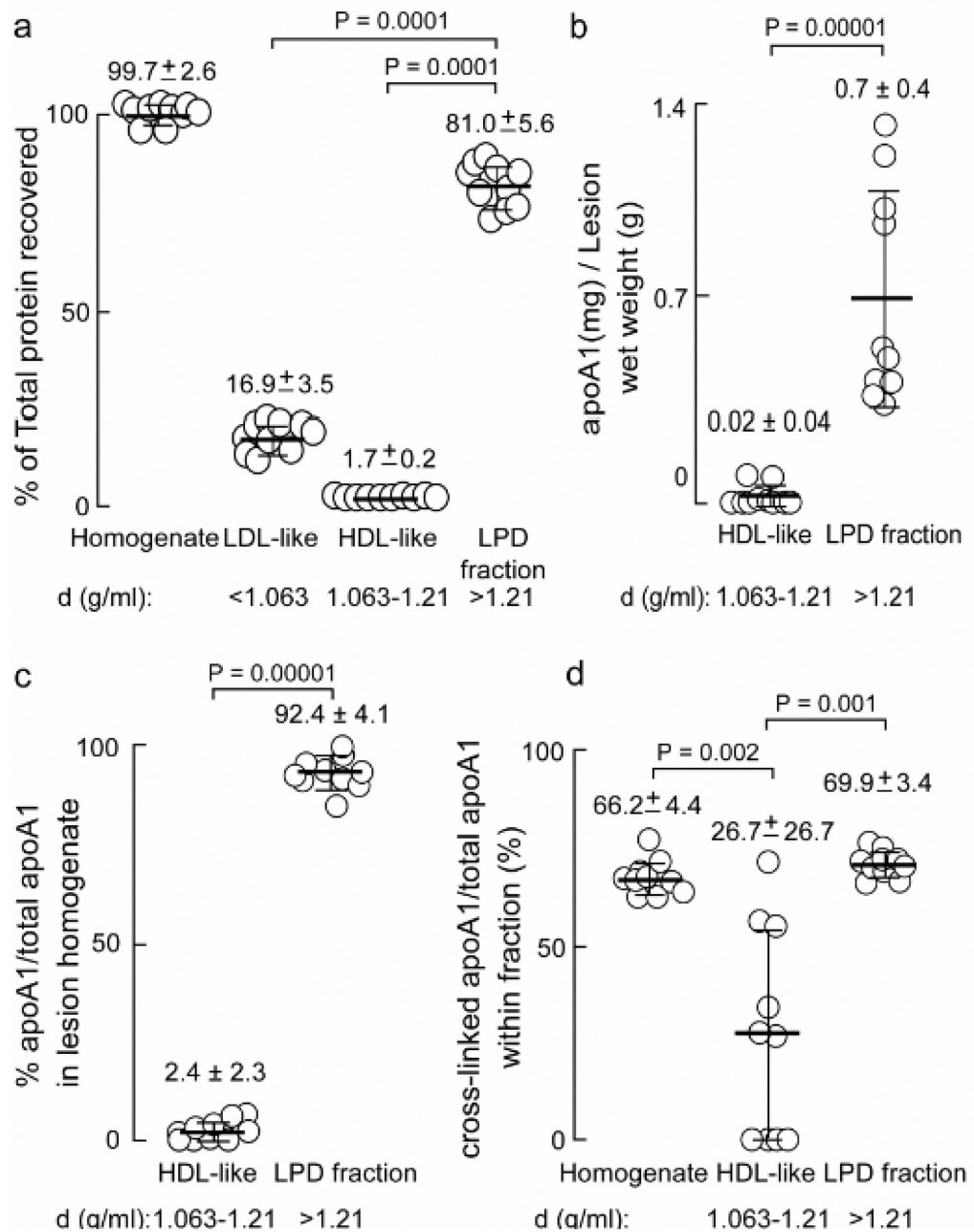


Figure 2.

ApoA1 from human atherosclerotic lesions is not located on HDL-like particles and is heavily cross-linked. Proteins in atherosclerotic lesion homogenate or after buoyant density ultracentrifugation fractionation into HDL-like particle and lipoprotein depleted fractions from the indicated density ranges were separated on 5–15% reducing SDS-PAGE gels. **a**, Sypro Ruby stained gel of the indicated protein samples (10 μ g) from homogenate and the indicated density ranges obtained from different atherosclerotic lesion tissue samples (n=5). **b**, Western blot membrane of a duplicate run gel as in panel a with 2.4 μ g, 0.4 μ g and 2.4 μ g of homogenate, HDL-like and LPD fraction proteins respectively, probed with anti-total apoA1

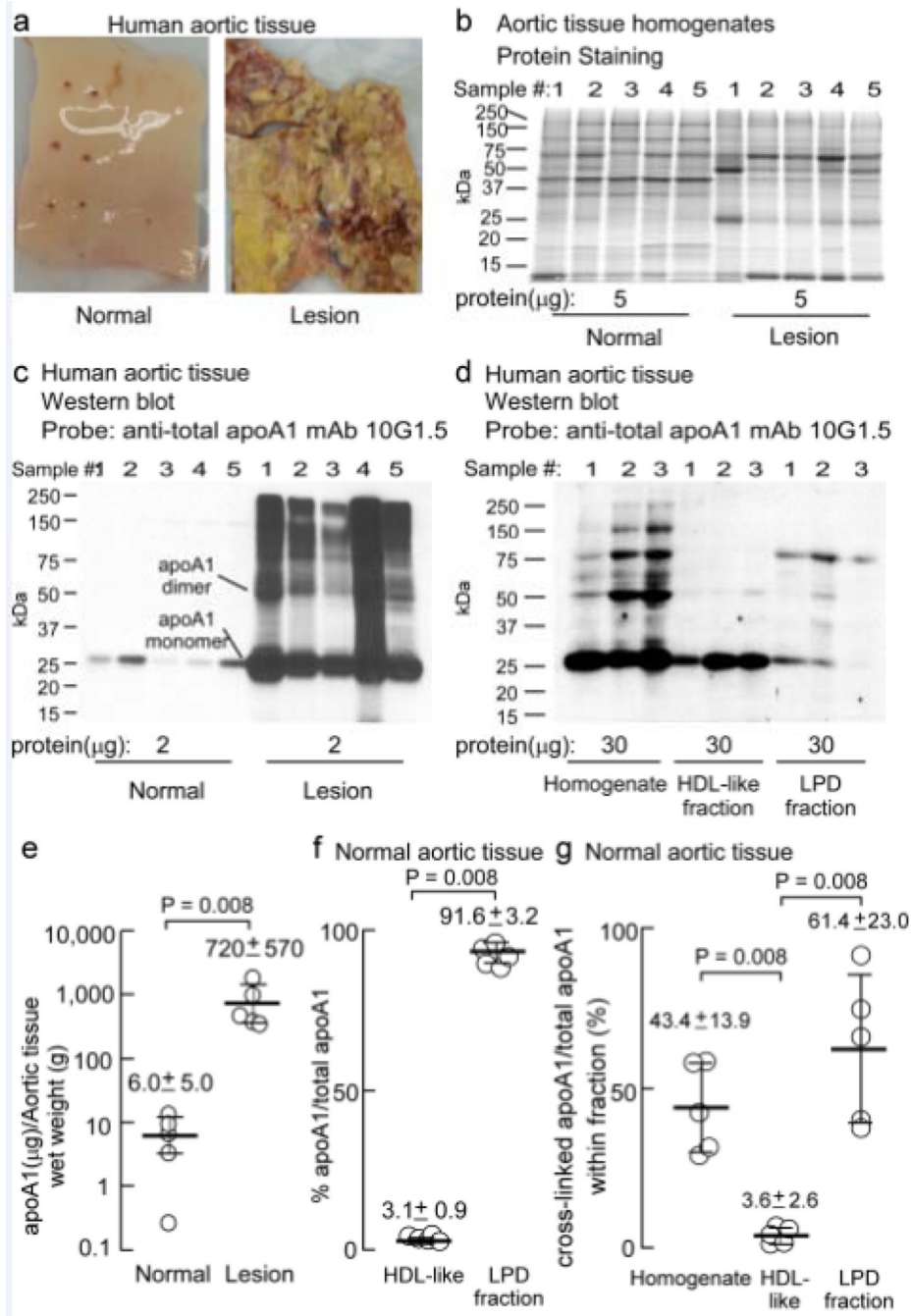
mAb 10G1.5. **c**, Overexposure of western blot in panel b to show apoA1 in HDL-like fraction. Monomeric and dimeric apoA1 immuno-reactive bands and Molecular weight markers are indicated.

Atherosclerotic Plaque-Laden Aorta

**Figure 3.**

Particle distribution of apoA1 obtained from human atherosclerotic artery wall. **a**, Percent of total protein in starting homogenate and in buoyant density ultracentrifugation fractions LDL-like, HDL-like and LPD determined by BCA protein assay are indicated. **b**, ApoA1 (mg) recovered per gram of lesion tissue (wet weight) in the HDL-like and LPD fractions; **c**, percent apoA1 to total apoA1 from atherosclerotic lesion homogenate present in the HDL-like and LPD fractions; **d**, cross-linked apoA1/total apoA1 within each fraction as a percentage was determined by quantitative western blot analysis of apoA1 immuno-reactive bands in Figure 2b and additional blots (not shown). Values were determined from samples

(n=10), error bars represent S.D. Mean values are indicated by a heavy horizontal line. Kruskal-Wallis test was used in panels (a) and (d) and found to be significant (P=0.0001 and P=0.0003 respectively). Dunn's test was used to adjust for multiple comparisons and Wilcoxon Rank Sum test was used in pairwise comparisons. Actual P values are listed when P<0.05.

**Figure 4.**

ApoA1 obtained from the artery wall is not on an HDL-like particle and behaves similarly to that isolated from atherosclerotic lesions. **a**, Representative aortic tissue from normal and atherosclerotic human artery wall. **b**, Sypro Ruby stained 5–15% SDS-PAGE gel of normal and atherosclerotic lesion homogenate ($n=5$) proteins (5 μ g). **c**, Western blot of duplicate gel as in panel a with the indicated amount of protein per lane ($n=5$) probed with anti-total apoA1 mAb 10G1.5. **d**, Western blot of normal artery wall proteins (30 μ g) from homogenate (sample 1, pooled samples 2&3 and pooled samples 4&5), HDL-like and LPD fractions probed with α -total apoA1 mAb 10G1.5 to show apoA1 and cross-linked apoA1. **e**,

ApoA1 (mg) recovered per gram of normal aortic tissue (wet weight) in the HDL-like and LPD fractions; **f**, apoA1 to total apoA1 as a percentage from normal aortic tissue homogenate present in the HDL-like and LPD fractions; **g**, cross-linked apoA1/total apoA1 within each fraction as a percentage was determined by quantitative western blot analysis of apoA1 immuno-reactive bands in panels (c) and (d). Monomeric and dimeric apoA1 are indicated. Values were determined from samples (n=5) in (c) and n=3 in (d) and additional blots (not shown), error bars represent S.D. Mean values are indicated by a heavy horizontal line. Kruskal-Wallis test was used in panel (g) and found to be significant (P=0.006). Wilcoxon Rank Sum test was used in pairwise comparisons to determine statistical differences. Actual P values are listed when P<0.05.

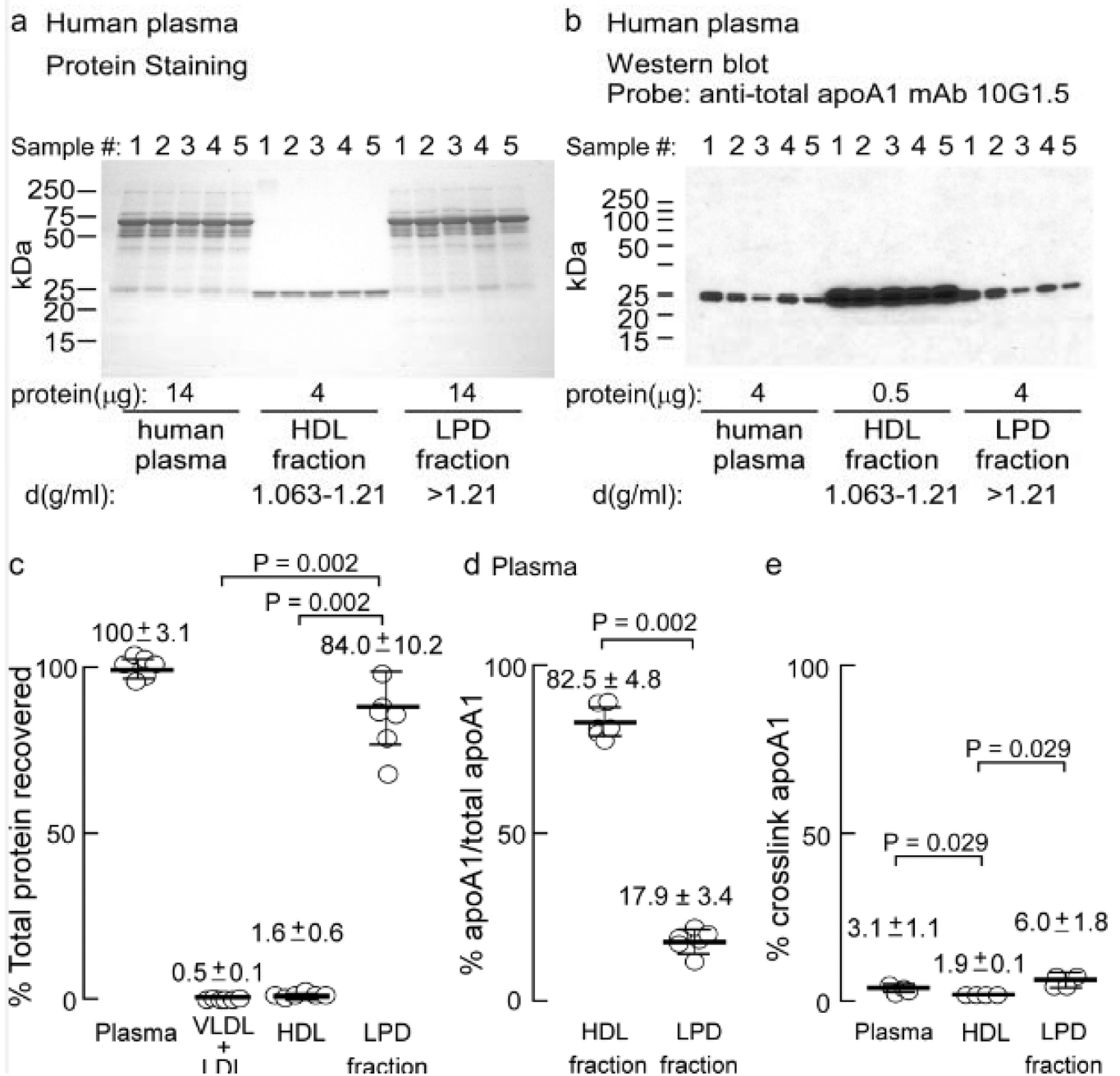


Figure 5. ApoA1 in plasma is on HDL particles and behaves differently than artery wall derived apoA1. Plasma from normal healthy human volunteers ($n=5$) was fractionated by buoyant density gradient centrifugation. **a**, Coomassie Blue stained 5–15% SDS-PAGE gel of plasma, HDL- and LPD fraction proteins and **b**, Western blot analysis of proteins on membrane from a duplicate fractionated protein gel probed with anti-total apoA1 mAb 10G1.5 shows apoA1 predominately in the HDL fraction and not cross-linked. **c**, Percentage of total protein recovered in starting material, and in the VLDL + LDL, HDL-like and LPD fractions. Quantitative analyses of panel B and overexposed panel B reveal percentage of apoA1 to total apoA1 present in the plasma HDL and LPD fractions in **d**, and cross-linked

apoA1/total apoA1 within plasma, HDL and LPD fractions in **e**. Values (c,d) were determined from samples (n=5). Error bars represent S.D., and the mean is indicated by a heavy horizontal line. Kruskal-Wallis test was used to determine statistical differences for data presented in panels (c) and (e), which was found to be significant (P=0.0002 and P=0.01, respectively). Dunn's test was used to adjust for multiple comparisons in panel c and Wilcoxon Rank Sum test was then used for pairwise comparisons. Actual P values are listed.

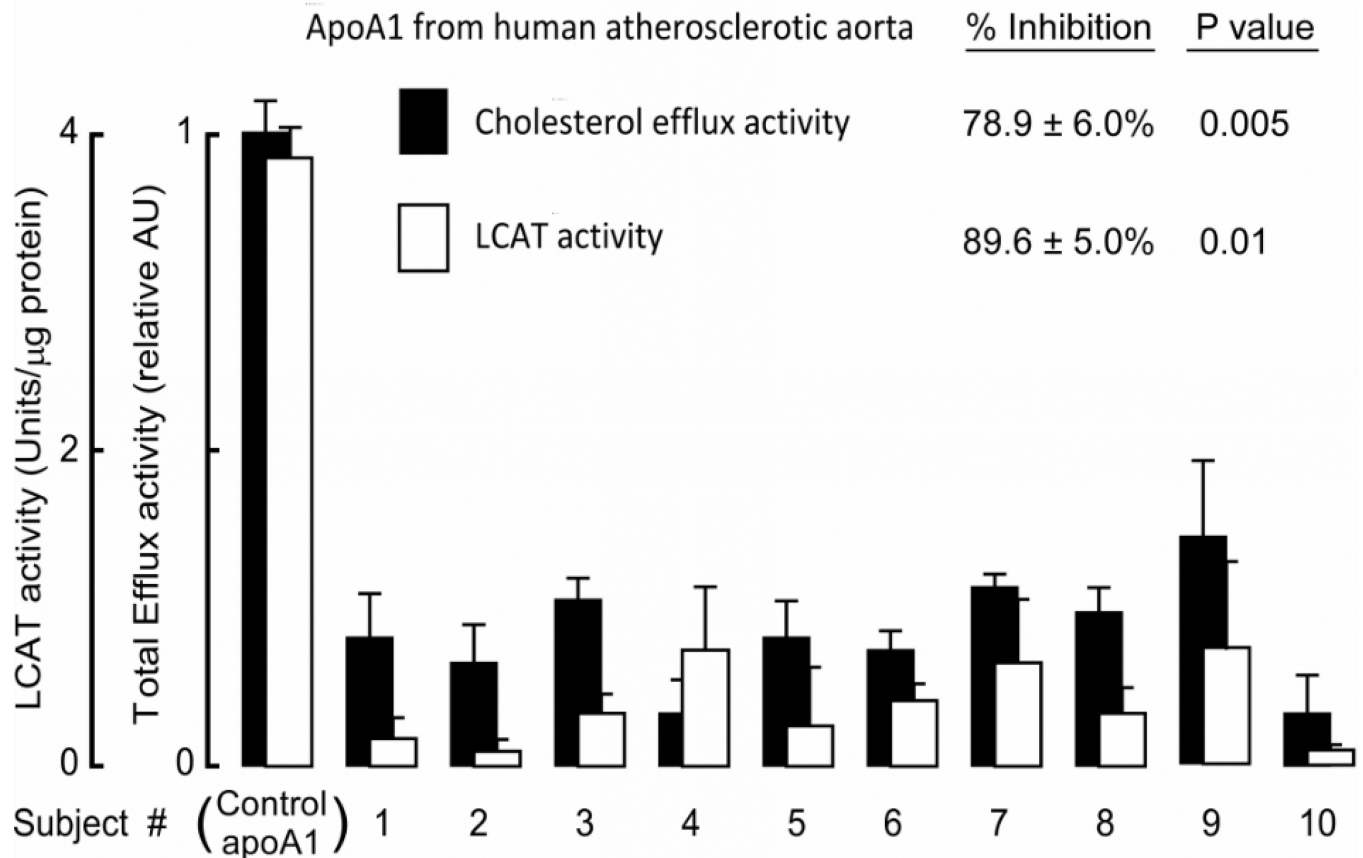


Figure 6.

Functional characterization of lesion apoA1. Macrophage cholesterol efflux activity, and LCAT activity, were measured in apoA1 immuno-affinity purified from human atherosclerotic-laden plaque (n=10 different subjects) as described under Methods. ApoA1 isolated from plasma HDL recovered from healthy donors (n=3) and rHDL formed from these apoA1 served as controls for total efflux activity, and LCAT activity, respectively. Bars represent triplicate determinations; error bars represent S.D. P values represent comparison between subject samples versus control apoA1 and were determined using the one-sample robust Hotelling T2 test.